

# Relationship between the Local Structures of Titanium Oxide Photocatalysts and Their Reactivities in the Decomposition of NO

Jinlong Zhang,<sup>†,‡</sup> Yun Hu,<sup>†</sup> Masaya Matsuoka,<sup>†</sup> Hiromi Yamashita,<sup>†</sup> Madoka Minagawa,<sup>†</sup> Hisao Hidaka,<sup>§</sup> and Masakazu Anpo<sup>\*,†</sup>

Department of Applied Chemistry, Graduate School of Engineering, Osaka Prefecture University, Gakuen-cho, Sakai, Osaka 599-8531, Japan, and Frontier Research Center for the Global Environment Protection, Meisei University, 2-1-1 Hodokubo, Hino, Tokyo 191, Japan

Received: May 31, 2001

Photocatalysts involving titanium oxides were prepared by an ion-exchange and impregnation method in which zeolites with different Si/Al ratios were used as supports. Those photocatalysts with low Si/Al ratios exhibited high and unique photocatalytic reactivity for the direct decomposition of NO into N<sub>2</sub>, O<sub>2</sub>, and N<sub>2</sub>O at 275 K. In situ photoluminescence, diffuse reflectance absorption, and XAFS investigations indicated that the titanium oxide species are highly dispersed within the zeolite and exist in tetrahedral coordination. The charge transfer excited state of these highly dispersed titanium oxide species plays a significant role in the decomposition of NO with a high selectivity for the formation of N<sub>2</sub> and O<sub>2</sub>, while the catalysts involving the aggregated octahedrally coordinated titanium oxide species show a high selectivity to produce N<sub>2</sub>O, being similar to the reactions observed on the powdered bulk TiO<sub>2</sub> photocatalysts.

## Introduction

In recent years, much attention has been focused on how to reduce NO from the air, and research into the removal of NO<sub>x</sub> is one of the most important and urgent fields of study.<sup>1–5</sup> Photocatalysis is a clean and attractive, low-temperature, nonenergy-intensive approach, significantly, for chemical waste remediation. Titanium oxide catalyst is one of the most investigated photocatalytic systems and has been found to be capable of decomposing a wide variety of organic and inorganic pollutants and toxic materials, in both liquid and gas-phase systems.<sup>6–8</sup> However, their reactivity and selectivity are not enough for large scale applications. On the other hand, highly dispersed titanium oxides prepared in zeolites or in silicalite cavities have also been found to exhibit unique and high photocatalytic reactivity in the reduction of CO<sub>2</sub> with H<sub>2</sub>O to produce CH<sub>3</sub>OH and CH<sub>4</sub>, as well as the direct decomposition of NO into N<sub>2</sub> and O<sub>2</sub>.<sup>6,9</sup> These photocatalytic reactions are very important with regard to reducing the greenhouse effect and controlling global air pollution as well as the development of highly active environmentally friendly and safe catalytic technologies using solar energy.<sup>4,6,9</sup>

To address the removal of nitrogen oxides (NO<sub>x</sub>,  $x = 1, 2$ ) from exhaust gases, semiconductors have been applied as photocatalysts which react under UV or visible light.<sup>4,6,9,10</sup> The design of molecular and/or cluster size titanium oxide photocatalysts within zeolite cavities and frameworks is of special interest because zeolites offer unique nanoscale pore reaction fields, an unusual internal surface topology, and ion-exchange capacities. The aim of the present work is to examine the

relationship between the photocatalytic properties of titanium oxides prepared within zeolites and the role of their local structures.

## Experimental Section

Ex.Ti/Y(x) and ex.Ti/ZSM-5 catalysts were prepared by an ion exchange method with an aqueous titanium ammonium oxalate solution using Y-zeolite samples (Si/Al = 5.6, 13.9 and 390) and ZSM-5 supplied by the TOSOH corporation.<sup>6</sup> Furthermore, the imp.Ti/ZSM-5 catalyst was prepared by impregnating ZSM-5 with an aqueous titanium ammonium oxalate.<sup>6</sup> The actual compositions of the photocatalysts were determined by atomic absorption. Samples were dissolved in an HF solution and measured on a Perkin-Elmer system with a sensitivity of 1.7 mg/mL.

The final catalysts were denoted as ex.Ti/Y(x), ex.Ti/ZSM-5, and imp.Ti/ZSM-5. TiO<sub>2</sub> powered catalysts (JRC-TIO-4; anatase 92%, rutile 8%) were supplied as a standard reference catalyst by the Catalysis Society of Japan. The photocatalytic reactions of NO molecules were carried out with the catalysts (100 mg) in a quartz cell with a flat bottom (60 mL) connected to a conventional vacuum system (10<sup>-6</sup> Torr range). Prior to photoreactions and spectroscopic measurements, the catalysts were degassed at 725 K for 2 h, heated in O<sub>2</sub> at the same temperature for 2 h, and finally evacuated at 475 K to 10<sup>-6</sup> Torr. UV irradiation of the catalysts in the presence of NO (7.8 μmol) was carried out using a 75 W high-pressure Hg lamp ( $\lambda > 280$  nm) at 275 K. The reaction products were analyzed by gas chromatography. The photoluminescence spectra of the catalysts were measured at 77 K using a Shimadzu RF-5000 spectrophotofluorometer. The UV absorption spectra were recorded with a Shimadzu UV-2200A spectrometer at 295 K. The XAFS spectra were measured at the BL-7C facility of the Photon Factory at the National Laboratory for High-Energy Physics, Tsukuba. The Ti K-edge absorption spectra were recorded in the transmission mode or fluorescence mode at 295

\* To whom correspondence should be addressed. E-mail: anpo@ok.chem.osakafu-u.ac.jp.

<sup>†</sup> Department of Applied Chemistry.

<sup>‡</sup> Permanent address: Institute of Fine Chemicals, East China University of Science and Technology, Shanghai 200237, P. R. China.

<sup>§</sup> Frontier Research Center for the Global Environment Protection.

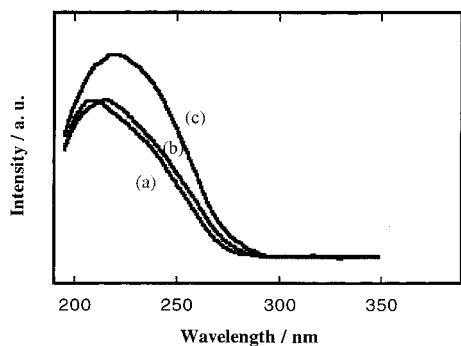


**Figure 1.** Diffuse reflectance UV-vis absorption spectra of ex.Ti/Y. (a) ex.Ti/Y(5.6), (b) ex.Ti/Y(13.9), and (c) ex.Ti/Y(390).

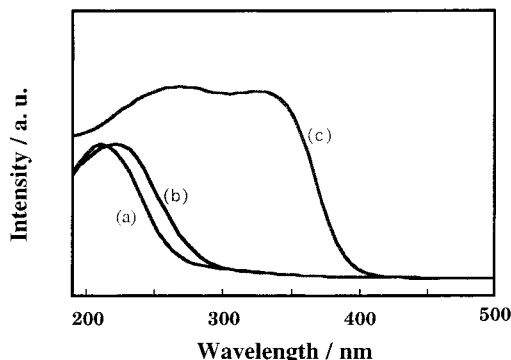


**Figure 2.** Diffuse reflectance UV-vis absorption spectra of the various Ti/ZSM-5 catalysts. (a) ex. Ti/ZSM-5(23.8), (b) imp. Ti/ZSM-5(23.8), and (c) P-25 as reference.

K. The normalized spectra were obtained by a procedure described in previous literature.<sup>11</sup>

## Results and Discussion

Figure 1 shows the diffuse reflectance UV spectra of the various photocatalysts. They were prepared by an ion-exchange method, and the Y-zeolite were used as supports, the Si/Al ratios of which were 5.6, 13.9, and 390, respectively. From Figure 1, it was observed that the UV absorption of the samples shifted to longer wavelengths with the increase in the ratio of Si/Al. This meant that the titanium oxide species became aggregated with the increase. As can be seen in Figure 2, the UV absorption spectrum of ex. Ti/ZSM-5 shifts to shorter wavelengths, and that of P-25 locates at the longest wavelength. The diffuse reflectance UV-vis spectra are usually considered to provide information on the coordination geometry of the Ti cation (the first coordination sphere) and the change in the ligands (the second coordination sphere) under various conditions.<sup>12</sup> Jorgensen<sup>13</sup> proposed that the LMCT transitions between the ligand ( $X = \text{H}-\text{O}-$ ,  $\text{Si}-\text{O}-$ ,  $\text{Ti}-\text{O}-$ , etc.) and the empty d orbital of  $\text{Ti}^{4+}$  can be estimated from the optical electronegativities  $\chi^{\circ}$  of ligand X and  $\text{Ti}^{4+}$  by the following equation:

$$\lambda = (1000/3)[\chi_{\text{opt}(X)} - \chi_{\text{opt}(\text{Ti})}]^{-1}$$

The increase in the coordination number of Ti from 4-fold to 6-fold increases the  $\chi_{\text{opt}(\text{Ti})}$  value from 1.85 to 2.0. Therefore, the LMCT band for Ti in the octahedral sites is located at a longer wavelength relative to Ti in the tetrahedral sites. The Ti atoms in either the anatase or rutile phase are located at the octahedral sites, and these results indicate that a single value of optical electronegativity may not properly represent the Ti atoms in the different coordination and ligand environments. Moreover, the electronegativity values used for oxygenated

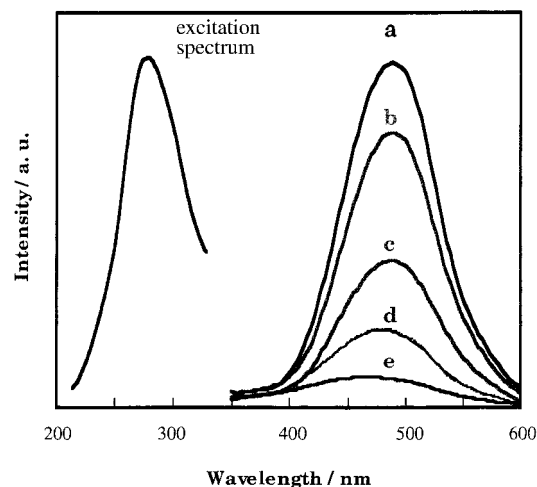
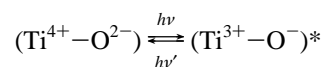


**Figure 3.** Effect of the addition of NO upon the photoluminescence spectrum of ex.Ti/Y (5.6) catalyst. (a) 0 Torr, (b) 0.1 Torr, (c) 3.2 Torr, (d) 6 Torr, and (e) 8 Torr.

ligands having different second coordination spheres are quite arbitrary. Therefore, the above equation cannot be quantitatively used to account for the shift in the LMCT transitions of the Ti atoms upon changes in coordination and ligand environments. As can be seen in Figure 1, the transition from sample ex.Ti/Y(5.6) to ex.Ti/Y(13.9) and ex.Ti/Y(390) causes only a slight red shift of the LMCT transitions, indicating that the coordination geometry changes as well as any changes in the ligand due to the relatively minor contribution of the titanium to the shift in the LMCT transitions. From Figure 2, the significant red shift of the LMCT transitions and the decrease in the edge energy with the changing  $\text{TiO}_2$  loading methods from ex.Ti/ZSM-5 to imp.Ti/ZSM-5 and P-25 can be observed. The decrease in the edge energy of the LMCT transitions of the Ti atoms may be associated with the increase in the number of the nearest Ti atoms, which suggests the polymerization of the surface Ti atoms with the impregnation method. These results clearly suggest that the dispersion of the Ti oxide species on the catalyst prepared by an ion-exchange is higher than that of the catalysts prepared by impregnation methods. According to several studies,<sup>14</sup> the absorption shoulder at 260–270 nm can be attributed to the presence of site-isolated Ti atoms in penta- or octahedral coordination. The ex.Ti/Y-zeolite sample exhibited a photoluminescence spectrum at around 450–600 nm by excitation at around 280 nm at 77 K.

Figure 3 shows the typical photoluminescence observed on ex.Ti/Y-zeolite by excitation with UV light. The observed photoluminescence and absorption bands are in good agreement with those previously observed with the highly dispersed tetrahedrally coordinated titanium oxides prepared in silica matrices,<sup>15,16</sup> where the absorption of UV light at around 280 nm brings about an electron transfer from the lattice oxygen ( $\text{O}_1^{2-}$ ) to the titanium ion ( $\text{Ti}^{4+}$ ) to form a charge transfer excited state. We can, therefore, conclude that the observed photoluminescence spectrum is attributed to the radiative decay process from the charge transfer excited state formed in this way to the ground state of the highly dispersed titanium oxide species having a tetrahedral coordination, as shown in the following scheme:



The addition of NO onto the ex.Ti/Y-zeolite catalyst led to an

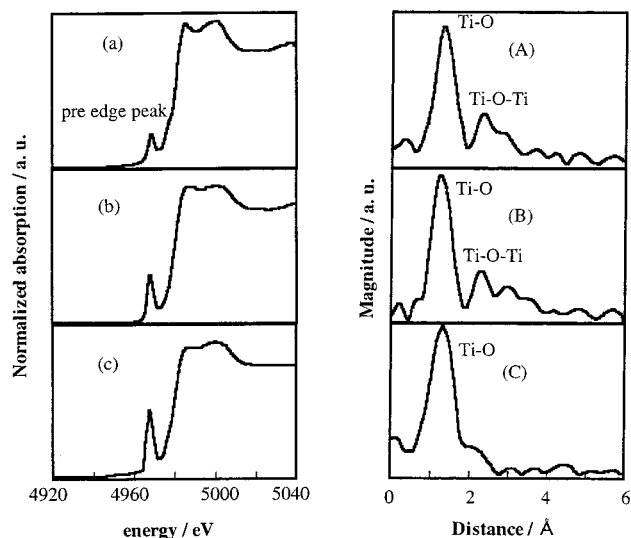


**Figure 4.** (a–c) XANES and (A–C) FT-EXAFS spectra of (a, A) ex. Ti/Y(390), (b, B) ex. Ti/Y(13.9), and (c, C) ex. Ti/Y(5.6).

efficient quenching of the photoluminescence spectrum of the catalyst, as shown in Figure 3. The intensity of the spectrum depended on the amount of NO added. The lifetime of the charge transfer excited state was also found to be shortened by the addition of NO. These results indicate not only that the tetrahedrally coordinated titanium oxide species locate at positions accessible to the added NO but also that the added NO easily interacts with the charge transfer excited state of the titanium oxide species.

The DRS results alone are insufficient to determine the coordination of Ti atoms because of the mixed contribution to the LMCT transitions from both coordination states and ligands. Combining the in situ DRS and XANES spectroscopies was found to provide the most direct and reliable structural information on the surface titanium oxide species.

The chemical structural information on the titanium oxide species within the zeolite is strongly dependent on the amount of Ti loading on the support. The edge region in the X-absorption spectra provides much information on the environment geometry and the electronic structure of the absorbing atom. Figure 4 shows the XANES spectra of three different samples used in this present work. The lack of inversion symmetry in the tetrahedral environment results in a single intense preedge peak. This peak is assigned to the allowed  $1s \rightarrow t_2$  transition for tetrahedral symmetry.<sup>17</sup> The intensities of the preedge peaks were in the following order: ex. Ti/Y-zeolite(5.6) > ex. Ti/Y-zeolite(13.9) > ex. Ti/Y-zeolite(390). The preedge features of the samples show differences with the increasing ratio of Si/Al in the catalysts, with the peak intensity in ex. Ti/Y-zeolite(5.6) being significantly higher, suggesting that the average coordination number of the Ti atoms is lower in samples with a lower ratio of Si/Al. As can be seen in Figure 4a for the ex. Ti/Y-zeolite(390), the single preedge peak is rather weak, indicating that the catalyst consists of a mixture of tetrahedrally and octahedrally coordinated oxide species. Previous literature<sup>18</sup> has shown that the preedge peak becomes less intense and wider, and shifts to a higher energy value when octahedral Ti is present in the form of an extraframework anatase or in systems with significant disorder in the Ti–O distances and Ti–O–Si angles.

Figure 4 also shows the FT-EXAFS spectra of the catalysts. All of the catalysts exhibit a strong peak at around 1.6 Å (without phase shift correction) which can be assigned to the

**TABLE 1: Comparisons of the Yields of N<sub>2</sub> and N<sub>2</sub>O and Their Selectivities in the Direct Photocatalytic Decomposition of NO at 275 K on the Various Types of the Ti/Zeolite Catalysts**

catalysts	Ti content (wt % as TiO <sub>2</sub> )	yields $\mu\text{mol/g}$ of TiO <sub>2</sub> h			selectivity (%)	
		N <sub>2</sub>	N <sub>2</sub> O	total	N <sub>2</sub>	N <sub>2</sub> O
ex. Ti/Y(5.6)	1.0	23	6	29	79	21
ex. Ti/Y(13.9)	1.0	19	7	26	73	27
ex. Ti/Y(390)	1.0	17	8	25	68	32
ex. Ti/ZSM-5	1.1	14	2	16	88	12
imp. Ti/ZSM-5	1.0	8	11	19	42	58
P-25		3	8	11	27	73

neighboring oxygen atoms (Ti–O). The ex. Ti/Y(5.6) exhibits only a Ti–O peak, indicating the presence of an isolated titanium oxide species, while the ex. Ti/Y(390) exhibits an intense peak at around 2.7 Å. This peak can be assigned to the aggregation of the titanium oxide species in the catalyst. From these results, it can be seen that ex. Ti/Y(5.6) contains isolated four-coordinate titanium ions. On the other hand, in the ex. Ti/Y(390), the presence of the aggregated octahedral titanium oxide species was clearly suggested.

UV irradiation of the ex. Ti/Y-zeolite(5.6), ex. Ti/Y-zeolite(13.9), ex. Ti/Y-zeolite(390), ex. Ti/ZSM-5, and imp. Ti/ZSM-5 photocatalysts in the presence of NO was found to lead to the evolution of N<sub>2</sub>, O<sub>2</sub>, and N<sub>2</sub>O in the gas phase at 275 K with different yields and different product selectivities. The yields of these photoformed N<sub>2</sub>, O<sub>2</sub>, and N<sub>2</sub>O increased linearly to the UV irradiation time and the reaction immediately stopped when irradiation was ceased. The formation of these reaction products was not detected under dark conditions nor in UV irradiation of the zeolites without titanium.

The photocatalytic reactivities of various titanium oxide catalysts for the direct decomposition of NO into N<sub>2</sub> and O<sub>2</sub> are shown in Table 1. Table 1 also shows the yields of the photoformed N<sub>2</sub> (O<sub>2</sub>) and N<sub>2</sub>O (efficiency) and their selectivity to produce N<sub>2</sub> in decomposition of NO. From Table 1, it is clear that the efficiency and selectivity for the formation of N<sub>2</sub> strongly depend on the type of catalyst. It was observed that the photocatalytic reactivity and selectivity for the formation of N<sub>2</sub> are much higher in low ratios than for high ratios of Si/Al.

Of special interest is the comparison of the photocatalytic reactivities of ex. Ti/ZSM-5 catalysts with that of imp. Ti/ZSM-5 in Table 1. The photocatalytic performance of the titanium oxide appears to be completely modified by its incorporation into the ZSM-5 zeolite, which is also associated with changes in the molecular structure and coordination environment. The unique catalytic performance of the highly dispersed titanium photocatalyst, ex. Ti/ZSM-5, in comparison with the aggregated titanium oxide photocatalyst shows higher photocatalytic reactivity and selectivity for the formation of N<sub>2</sub> and O<sub>2</sub>. It is thus clear that the selectivity for the formation of N<sub>2</sub> is much higher when prepared by an ion-exchange method than by an impregnation method. Moreover, the catalytic activity and selectivity for the formation of N<sub>2</sub> are associated with changes in the coordination geometry and the degree of the polymerization of the surface titanium oxide species. From these results, it was found that the photocatalytic reactivity and selectivity for the formation of N<sub>2</sub> decrease with an increase in the aggregated titanium oxides in the photocatalysts. Polymerization of the titanium oxide species when the titanium oxide are loaded by an impregnation method leads to a decrease in the fraction of the Ti–O–Si bonds and, therefore, significantly decreases the photocatalytic reactivity of the catalyst. Thus, in the case of

the highly dispersed tetrahedrally coordinated  $\text{TiO}_4$  species, under UV irradiation, two NO molecules can be activated on a photoexcited  $\text{TiO}_4$  species, resulting in the formation of  $\text{N}_2$  and  $\text{O}_2$ .<sup>3</sup> Meanwhile, in the case of the aggregated octahedrally coordinated titanium oxide particles, the photoformed electrons and holes react with NO molecules at different sites, respectively, and this situation results in the formation of  $\text{NO}_2$  and/or  $\text{N}_2\text{O}$  but not  $\text{N}_2$  and  $\text{O}_2$ , since N and O formed in the primary processes of the decomposition of NO immediately react with another NO molecules to form  $\text{NO}_2$  and  $\text{N}_2\text{O}$ . Thus, the photocatalytic reaction mechanism on the highly dispersed isolated tetrahedrally coordinated  $\text{TiO}_4$  species is completely different from the mechanism operating on titanium oxide semiconductor particles.<sup>2-3,19</sup>

## Conclusions

The results obtained by combined in situ UV-vis spectra, photoluminescence, and XAFS spectroscopies were very important for a fundamental understanding of the chemical structures of the ex.Ti/Y-zeolite with different ratios of Si/Al. The chemical structures of these photocatalysts were found to be very sensitive to different environments. For a sample with low Si/Al ratios, the surface Ti atoms were predominantly located at isolated titanium oxide species, existed in tetrahedral coordination, while with an increase in the ratio of Si/Al, the photocatalysts consisted of mixture of the tetrahedral and octahedral coordinated titanium oxide species. These results showed that a high photocatalytic efficiency and selectivity for the formation of  $\text{N}_2$  in the photocatalytic decomposition of NO could be achieved with the ex.Ti/Y-zeolite(5.6) catalyst having a highly dispersed isolated tetrahedral titanium oxide species, and the reactivity decreased with an increase in the Si/Al ratio. The selectivity for the formation of  $\text{N}_2\text{O}$  in the photocatalytic decomposition of NO was found to increase on imp-Ti/ZSM-5 as well as the photocatalysts with the higher Si/Al ratios which involve the aggregated octahedrally coordinated titanium oxide species.

**Acknowledgment.** The present work has been supported in part by the Ministry of Education of Japan, Grant-in-Aid for JSPS Fellows (Grant 98096).

## References and Notes

- (1) Notari, B. *Adv. Catal.* **1996**, *41*, 253 and references therein.
- (2) Anpo, M. *Catal. Surv. Jpn.* **1997**, *1*, 169 and references therein.
- (3) Anpo, M.; Che, M. *Adv. Catal.* **1999**, *44*, 116 and references therein.
- (4) Anpo, M.; Ed. *Photofunctional Zeolites*, Nova Science: Huntington, NY, 2000 and references therein.
- (5) Janssen, F. J. In *Handbook of Heterogeneous Catalysis*; Ertl, G., Knozinger, H., Weitkamp, J., Eds.; VCH: Weinheim, 1997; Vol. 4, p 1633.
- (6) Yamashita, H.; Ichihashi, Y.; Anpo, M.; Hashimoto, M.; Louis, C.; Che, M. *J. Phys. Chem.* **1996**, *100*, 16042.
- (7) Anpo, M.; Ichihashi, Y.; Takeuchi, M.; Yamashita, H. *Res. Chem. Intermed.* **1998**, *24*, 143.
- (8) Zhang, Z.; Wang, C-C.; Zakaria, R.; Ying, J. Y. *J. Phys. Chem. B.* **1998**, *102*, 10871.
- (9) Anpo, M.; Yamashita, H. In *Heterogeneous Photocatalysis*; Schiavello, M., Ed.; Wiley & Sons: London, 1997; p131.
- (10) Yamashita, H.; Honda, M.; Harada, M.; Ichihashi, Y.; Anpo, M.; Hiro, T.; Itoh, N.; Iwamoto, N. *J. Phys. Chem. B.* **1998**, *102*, 10707.
- (11) Tanaka, T.; Yamashita, H.; Tsuchitani, R.; Funabiki, T.; Yoshida, S. *J. Chem. Soc., Faraday Trans. 1* **1988**, *84*, 2987.
- (12) Gao, X.; Bare, S. R.; Fierro, J. L. G.; Banares, M. A.; Wachs, I. E. *J. Phys. Chem. B.* **1998**, *102*, 5653.
- (13) Jorgensen, C. K.; *Morden Aspects of Ligand Field Theory*; North-Holland: Amsterdam, 1971.
- (14) Trong On, D.; Denis, I.; Lortie, C.; Cartier, C.; Bonnevier, L. *Stud. Surf. Sci. Catal.* **1994**, *83*, 101.
- (15) Anpo, M.; Chiba, K. *J. Mol. Catal.* **1992**, *74*, 207.
- (16) Yamashita, H.; Ichihashi, Y.; Harada, M.; Stewart, G.; Fox M. A.; Anpo, M. *J. Catal.* **1996**, *158*, 97.
- (17) Blasco, T.; Cambor, M. A.; Corma, A.; Perez-Pariente, J. *J. Am. Chem. Soc.* **1993**, *115*, 11806.
- (18) Blasco, T.; Cambor, M. A.; Corma, A.; Esteve, P.; Guil, J. M.; Martinez, A.; Perdigon-Melon, J. A.; Valencia, S. *J. Phys. Chem. B.* **1998**, *102*, 75.
- (19) Anpo, M.; Aikawa, N.; Kubokawa, Y.; Che, M.; Louis, C.; Giamello, E. *J. Phys. Chem. B.* **1985**, *89*, 5017.
- (20) Anpo, M.; Nakaya, H.; Kodama, S.; Kubokawa, Y.; Domen, K.; Onishi, T. *J. Phys. Chem. B.* **1986**, *90*, 1633.
- (21) Anpo, M. *Res. Chem. Intermed.* **1989**, *11*, 67.